

# The extremotolerant desert moss *Syntrichia caninervis* is a promising pioneer plant for colonizing extraterrestrial environments

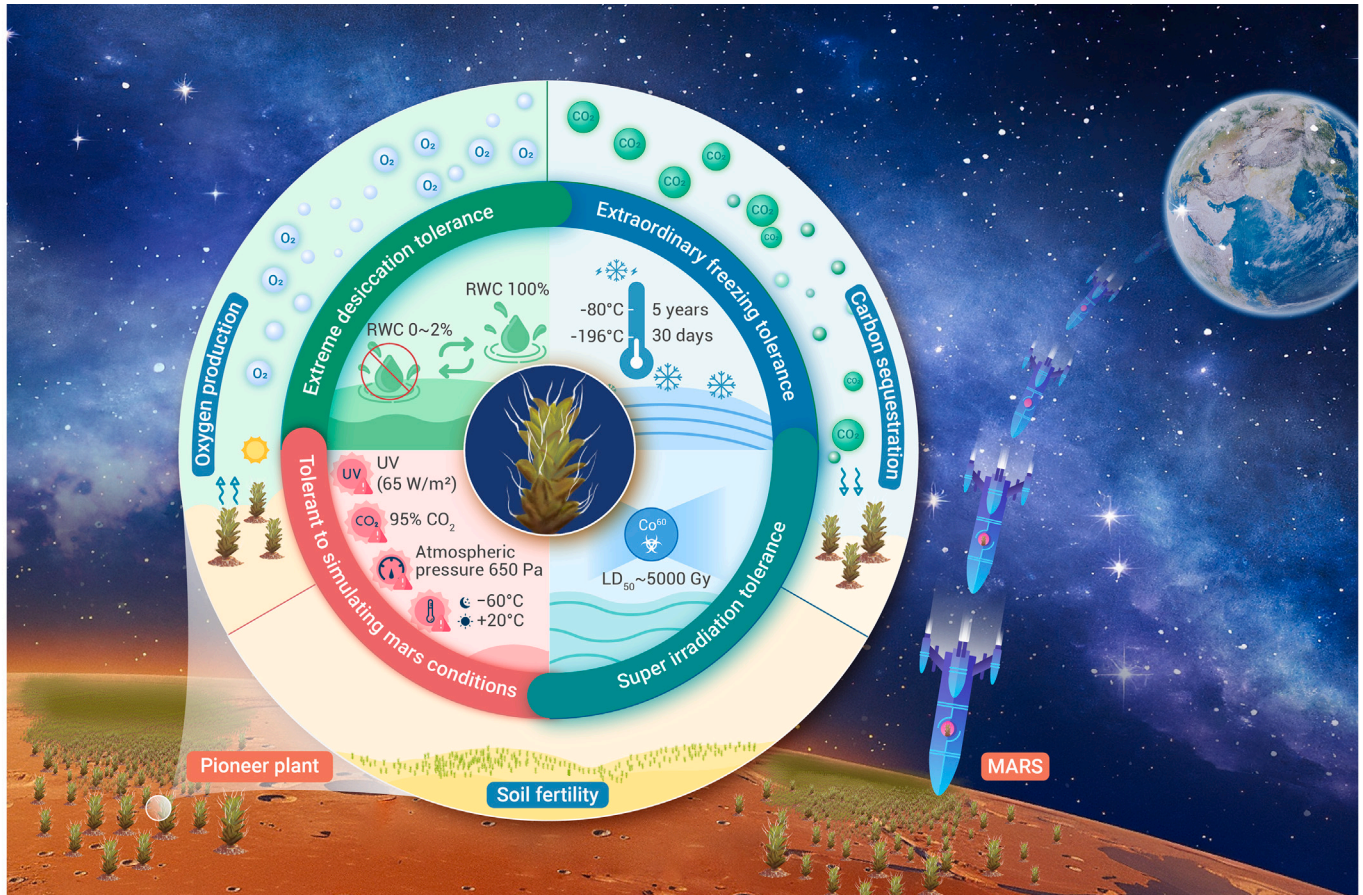
Xiaoshuang Li,<sup>1</sup> Wenwan Bai,<sup>1,2</sup> Qilin Yang,<sup>1,2</sup> Benfeng Yin,<sup>1</sup> Zhenlong Zhang,<sup>3</sup> Banchi Zhao,<sup>3</sup> Tingyun Kuang,<sup>4,\*</sup> Yuanming Zhang,<sup>1,\*</sup> and Daoyuan Zhang<sup>1,\*</sup>

\*Correspondence: [kuangty@ibcas.ac.cn](mailto:kuangty@ibcas.ac.cn) (T.K.); [zhangym@ms.xjb.ac.cn](mailto:zhangym@ms.xjb.ac.cn) (Y.Z.); [zhangdy@ms.xjb.ac.cn](mailto:zhangdy@ms.xjb.ac.cn) (D.Z.)

Received: April 16, 2024; Accepted: June 8, 2024; Published Online: June 30, 2024; <https://doi.org/10.1016/j.xinn.2024.100657>

© 2024 Published by Elsevier Inc. on behalf of Youth Innovation Co., Ltd. This is an open access article under the CC BY-NC-ND license (<http://creativecommons.org/licenses/by-nc-nd/4.0/>).

## GRAPHICAL ABSTRACT



## PUBLIC SUMMARY

- Extreme desiccation tolerance: recover within seconds after >98% water loss.
- Extraordinary freezing tolerance: withstand  $-196^{\circ}\text{C}$  ultra-low temperature.
- Super resistance to gamma radiation: with half-lethal dose estimated to be 5,000 Gy.
- This desert moss can survive and maintain vitality in simulated Mars conditions.
- The extremotolerant moss is a promising pioneer for Mars colonization.



# The extremotolerant desert moss *Syntrichia caninervis* is a promising pioneer plant for colonizing extraterrestrial environments

Xiaoshuang Li,<sup>1</sup> Wenwan Bai,<sup>1,2</sup> Qilin Yang,<sup>1,2</sup> Benfeng Yin,<sup>1</sup> Zhenlong Zhang,<sup>3</sup> Banchi Zhao,<sup>3</sup> Tingyun Kuang,<sup>4,\*</sup> Yuanming Zhang,<sup>1,\*</sup> and Daoyuan Zhang<sup>1,\*</sup>

<sup>1</sup>State Key Laboratory of Desert and Oasis Ecology, Key Laboratory of Ecological Safety and Sustainable Development in Arid Lands, Xinjiang Institute of Ecology and Geography, Chinese Academy of Sciences, Urumqi 830011, China

<sup>2</sup>University of Chinese Academy of Sciences, Beijing 100049, China

<sup>3</sup>National Space Science Center, Chinese Academy of Sciences, Beijing 100190, China

<sup>4</sup>Institute of Botany, Chinese Academy of Sciences, Beijing 100093, China

\*Correspondence: [kuangty@ibcas.ac.cn](mailto:kuangty@ibcas.ac.cn) (T.K.); [zhangym@ms.xjb.ac.cn](mailto:zhangym@ms.xjb.ac.cn) (Y.Z.); [zhangdy@ms.xjb.ac.cn](mailto:zhangdy@ms.xjb.ac.cn) (D.Z.)

Received: April 16, 2024; Accepted: June 8, 2024; Published Online: June 30, 2024; <https://doi.org/10.1016/j.xinn.2024.100657>

© 2024 Published by Elsevier Inc. on behalf of Youth Innovation Co., Ltd. This is an open access article under the CC BY-NC-ND license (<http://creativecommons.org/licenses/by-nc-nd/4.0/>).

Citation: Li X., Bai W., Yang Q., et al., (2024). The extremotolerant desert moss *Syntrichia caninervis* is a promising pioneer plant for colonizing extraterrestrial environments.

The Innovation **5(4)**, 100657.

Many plans to establish human settlements on other planets focus on adapting crops to growth in controlled environments. However, these settlements will also require pioneer plants that can grow in the soils and harsh conditions found in extraterrestrial environments, such as those on Mars. Here, we report the extraordinary environmental resilience of *Syntrichia caninervis*, a desert moss that thrives in various extreme environments. *S. caninervis* has remarkable desiccation tolerance; even after losing >98% of its cellular water content, it can recover photosynthetic and physiological activities within seconds after rehydration. Intact plants can tolerate ultra-low temperatures and regenerate even after being stored in a freezer at  $-80^{\circ}\text{C}$  for 5 years or in liquid nitrogen for 1 month. *S. caninervis* also has super-resistance to gamma irradiation and can survive and maintain vitality in simulated Mars conditions; i.e., when simultaneously exposed to an anoxic atmosphere, extreme desiccation, low temperatures, and intense UV radiation. Our study shows that *S. caninervis* is among the most stress tolerant organisms. This work provides fundamental insights into the multi-stress tolerance of the desert moss *S. caninervis*, a promising candidate pioneer plant for colonizing extraterrestrial environments, laying the foundation for building biologically sustainable human habitats beyond Earth.

## INTRODUCTION

Exploring and colonizing extraterrestrial environments is an ambitious goal that may improve long-term human sustainability.<sup>1–3</sup> Mars is considered to be the most likely planet for future human colonization.<sup>4–7</sup> No life forms have been detected on Mars to date. Therefore, introducing organisms from Earth might be required to produce Earth-like conditions suitable for human life on Mars, a process known as terraforming.<sup>8</sup> Terraforming will require the selection of suitable organisms from Earth or the engineering of novel organisms (particularly plants) that can thrive in challenging extraterrestrial conditions. To date, only a few studies have focused on testing the ability of organisms to withstand the extreme environments of outer space or Mars. These studies have primarily focused on microorganisms,<sup>9–13</sup> algae,<sup>8</sup> and lichens.<sup>14–16</sup> However, plants such as mosses offer key benefits for terraforming, including stress tolerance, a high capacity for photoautotrophic growth, and the potential to produce substantial amounts of biomass under challenging conditions.

Studies of challenging environments on Earth can inform the selection of plants for growth in extraterrestrial environments. The biological soil crust (BSC) is a widespread type of ground cover often found in arid lands. The BSC consists of organic complexes of cryptogamic plants such as lichens and mosses, microbes such as cyanobacteria, and the secretions from these organisms that become mixed with soil particles.<sup>17</sup> The BSC serves as a pioneer substrate in vegetative succession due to its remarkable resilience to intense radiation and its ability to withstand drought and other extreme environmental factors.<sup>18,19</sup> This has led to the widespread distribution of the BSC in global desert regions, with up to 70% coverage in some areas.<sup>20,21</sup> The BSC significantly enhances the water-holding capacity and structural stability of the underlying sand.<sup>20,22–24</sup> Moreover, the BSC is a major source of carbon and nitrogen in arid regions, accounting for one-fourth of the total biological nitrogen fixation of terrestrial ecosystems worldwide.<sup>25,26</sup> Therefore, the BSC has been referred

to as the “living skin” of the Earth, as it plays crucial roles in modulating hydrology, nutrient cycling, and other essential ecological processes.

Among land plants, mosses are often the pioneer species that are naturally selected for growth in extreme environments. Moss crusts represent an advanced stage in the development of BSCs. Compared with algae and lichen crusts, moss crusts have greater biomass and carbon fixation capacity, thus playing important roles in biogeochemical cycles and stabilizing the desert surface.<sup>27–29</sup> *Syntrichia caninervis*, a common, dominant species in moss crust, possesses remarkable tolerance to multiple environmental stress factors (drought, cold, and radiation), giving it a great ecological advantage in harsh natural habitats.<sup>30</sup> *S. caninervis* has a widespread global distribution, as evidenced by geographical data from field surveys and the Global Biodiversity Information Facility database (Figure 1A). *S. caninervis* crusts are predominant in dryland regions, including the Gurbantunggut and Tengger Deserts in China and the Mojave Desert in the United States. *S. caninervis* crusts are also present in mountainous regions of the Pamir, Tibet, Middle East, Antarctica, and circumpolar regions.<sup>30</sup> The Gurbantunggut Desert in northwest China has one of the most concentrated distributions of *S. caninervis* worldwide (Figure 1B). Based on meteorological monitoring from 2005 to 2023, the lowest and highest temperatures in this desert were nearly  $-40^{\circ}\text{C}$  and  $65^{\circ}\text{C}$ , respectively, and the relative humidity was as low as 1.4%.

This extreme climate has shaped the remarkable resilience of *S. caninervis* to various environmental factors. *S. caninervis* plants exhibit extreme desiccation tolerance, usually appearing black when in a completely dry state in the wild after losing more than 98% of their water (Figure 1C). Notably, desiccated plants turn green and rapidly recover their photosynthetic capacity within seconds of rehydration (Figure 1D).<sup>31</sup> *S. caninervis* has evolved several morphological mechanisms to adapt to extreme environments, including overlapping leaves that conserve water and shield the plant from intense sunlight and white awns at the tops of leaves that reflect strong solar radiation and enhance water utilization efficiency (Figures 1D and 2B).<sup>32</sup> Moreover, these plants remain photosynthetically active under snow cover (Figure 1E) and can maintain vigorous growth, contributing up to 49% of their annual total carbon fixation during the frequent freeze-thaw cycles in spring.<sup>33–35</sup> *S. caninervis* also shows high tolerance to extremely low temperatures.

In this study, we evaluated the extraordinary resilience of *S. caninervis* under extreme desiccation, ultra-low temperatures, and intense radiation as well as in a simulated Martian environment combining several of these stress factors. The unique insights obtained in our study lay the foundation for outer space colonization using naturally selected plants adapted to extreme stress conditions.

## RESULTS

### Drying without dying

To explore the tolerance of *S. caninervis* to extreme desiccation, we subjected this moss to an air-drying regimen in the laboratory and recorded plant phenotypes, relative water content (RWC), optimal photochemical efficiency of photosystem II ( $F_v/F_m$ ), and changes in leaf angle. *S. caninervis* plants exhibited extreme desiccation tolerance, manifested by their capacity to undergo complete dehydration and very rapidly recover (Figure 2). The plants appeared green when saturated with water, turned dark green and then black as water was gradually lost, and turned green again only 2 s after rehydration (Figures 2A and 2B).

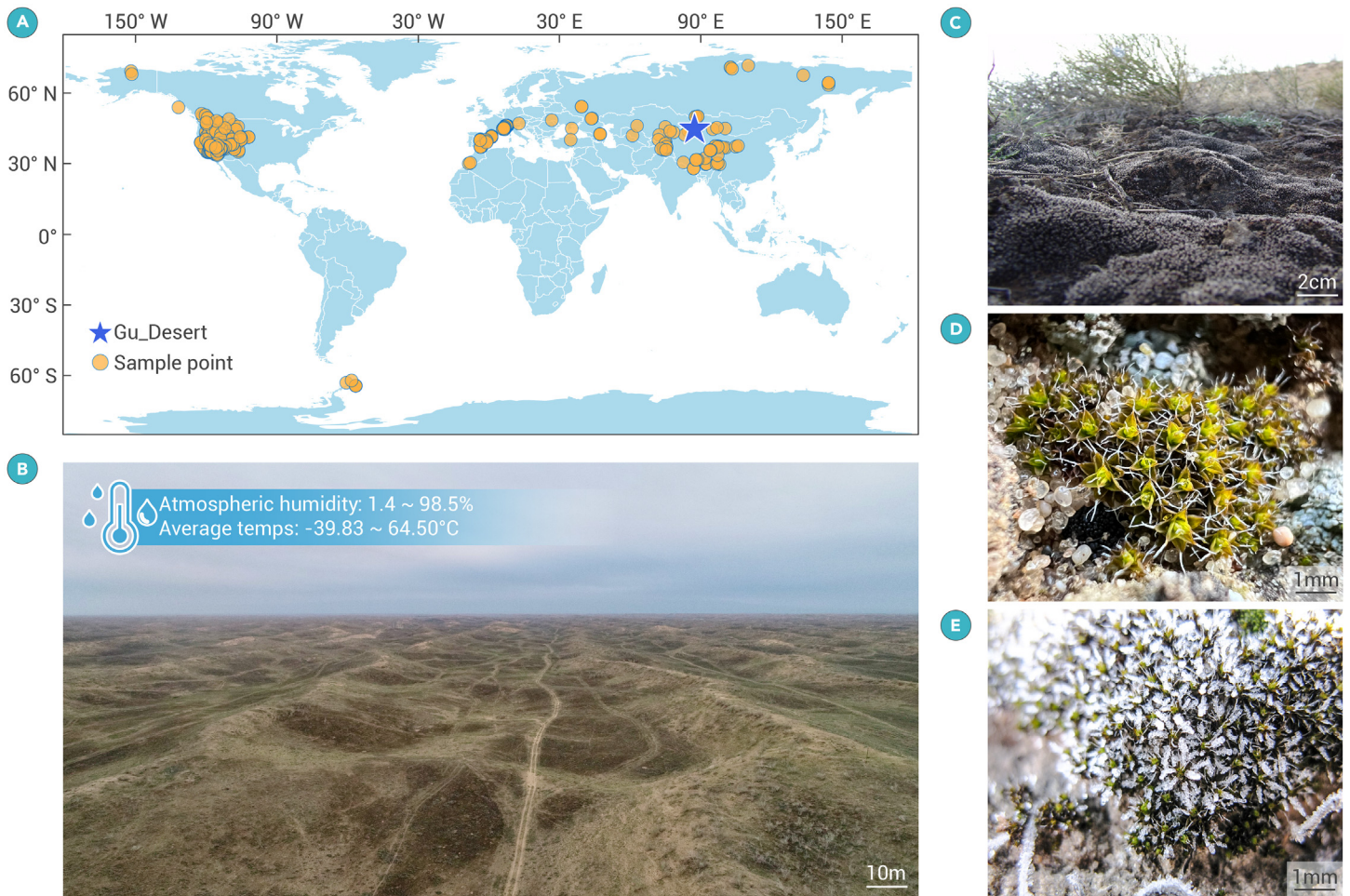


**Figure 1. Global distribution and different states of *S. caninervis* crust** (A) Global geographic distribution of *S. caninervis* crust. Database: Global Biodiversity Information Facility (<https://www.gbif.org/>). (B) A typical habitat where *S. caninervis* crust is found in the Gurbantunggut desert of China. Scale bar: 10 m. (C) Desiccated *S. caninervis* crust. Scale bar: 2 cm. (D) Hydrated *S. caninervis* crust. Scale bar: 1 mm. (E) Frozen *S. caninervis* crust with snow cover in winter. Scale bar: 1 mm.

The RWC decreased gradually and steadily as dehydration progressed, with over 40% of water lost in 10 min and more than 99% lost in 40 min. The RWC of dehydrated *S. caninervis* plants increased to more than 80% at 20 s of rehydration and was restored to 100% in 2 min (Figure 2C).

The  $F_v/F_m$  values, which represent photosynthetic capacity, decreased significantly as dehydration progressed, dropping by 54% after 20 min to nearly zero after 40 min of dehydration. Within 20 s of rehydration,  $F_v/F_m$  recovered rapidly to 65% of the initial level in hydrated plants and increased to the original level within 2 min (Figure 2D). During dehydration, the leaves became markedly curled and shrunken, and the leaf angles became smaller. During rehydration, the leaves stretched and recovered their original positions within 20 s (Figure 2E). Thus, *S. caninervis* plants can withstand extreme dehydration stress and have a robust ability to swiftly recover their physiological activities within seconds.

### Freezing without dying

To investigate the tolerance of *S. caninervis* plants to prolonged exposure to extremely low temperatures, we exposed completely dry (0%–2% RWC) and fully hydrated (100% RWC) plants to  $-80^\circ\text{C}$  in an ultra-low-temperature freezer for 3 or 5 years and to  $-196^\circ\text{C}$  (in a liquid nitrogen storage tank) for 15 or 30 days. The plants were transferred to sand for recovery and cultivated under normal growth conditions to observe their regeneration ability. The experimental design is illustrated in Figure 3A. Dry *S. caninervis* plants survived and regenerated new branches after these low-temperature treatments (Figure 3B). Without freezing treatment, the number of regenerated new branches in *S. caninervis* plants 5 days after rehydration was approximately 1–2 per plant and reached the maximum ( $\sim 3$ ) 30 days after rehydration.

After being exposed to  $-80^\circ\text{C}$  for 3 years, the number of regenerated new branches was  $0.22 \pm 0.15$  after 5 days of recovery (in sand under normal growth

conditions). The maximum branch number was slightly lower at 30 days of recovery ( $2.22 \pm 0.40$ ) (Figure 3C). After being exposed to  $-80^\circ\text{C}$  for 5 years, the number of regenerated new branches was  $0.10 \pm 0.10$  at 5 days of recovery, and the maximum branch number was  $1.90 \pm 0.18$ . During the recovery period, the number of regenerated new branches after 5 years of exposure to  $-80^\circ\text{C}$  was slightly, but not significantly, lower than after 3 years of  $-80^\circ\text{C}$  treatment (Figure 3C). For untreated plants, the regeneration rate after dehydration reached 75% on day 5 and 100% on day 15 after rehydration. For *S. caninervis* plants treated at  $-80^\circ\text{C}$  for 3 or 5 years, the regeneration rates were significantly lower than the control after 5 days of recovery (10% and 5%, respectively) but rose to approximately 90% after 30 days of recovery (Figure 3D).

Similar results were obtained for plants subjected to  $-196^\circ\text{C}$  treatment (Figures 3E–3G). Following 15 and 30 days of storage in liquid nitrogen, the plants ultimately regenerated approximately two new branches (Figure 3F); the regeneration rate was approximately 95% that of control plants (Figure 3G). We also applied the same low-temperature treatments to hydrated *S. caninervis* plants (RWC = 100%) and demonstrated that hydrated *S. caninervis* can also survive and maintain their regenerative ability following extreme freezing stress, although the number of new branches and rate of regeneration were lower than for plants frozen in a dry state (Figure S1).

### Radiation exposure without dying

For the gamma irradiation experiments, completely dry (0%–2% RWC) and fully hydrated (100% RWC) *S. caninervis* samples were exposed to total doses of 500 to 16,000 Gy, rehydrated, and transferred to sand for recovery and cultivation under normal growth conditions (Figure 4A). We detected dose-dependent effects on survival and regeneration (Figure 4B). For untreated control samples (0 Gy), following rehydration and a recovery period, the average

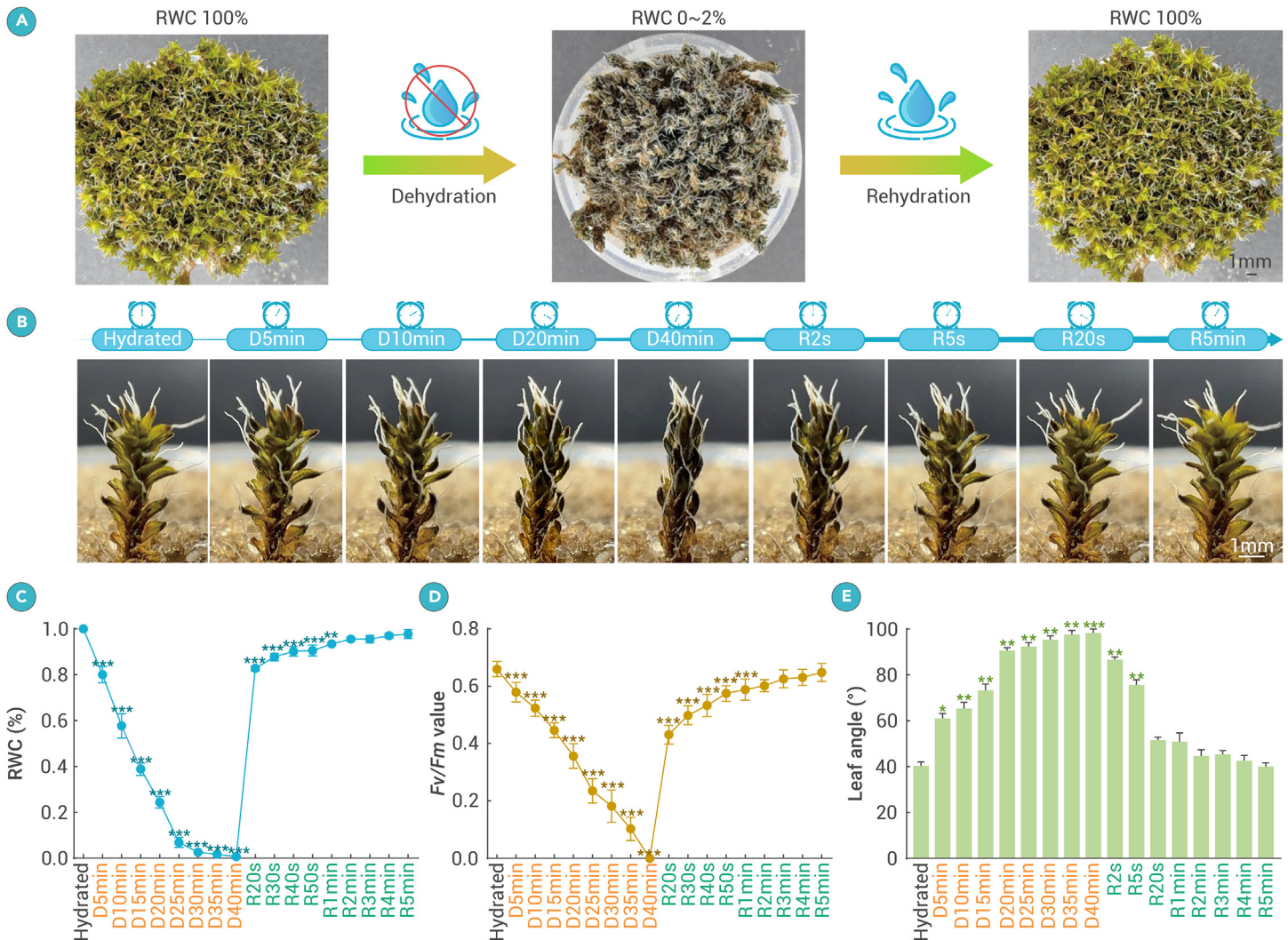


**Figure 2. Phenotypic changes and physiological responses of *S. caninervis* plants during the D-R process** (A) Phenotypic changes in *S. caninervis* crust during dehydration and subsequent rehydration. (B) Phenotypic changes in individual *S. caninervis* plants during dehydration (D) and rehydration (R). (C–E) Relative water content (RWC), optimal photochemical efficiency of photosystem II ( $F_v/F_m$ ), and changes in leaf angle of individual *S. caninervis*. Dry *S. caninervis* samples were fully hydrated with ultrapure water for 24 h and air dried in the laboratory (~30% relative humidity, 20°C–22°C) for dehydration treatment. Completely dry mosses were then watered to saturation for rehydration. At each treatment time point, a video camera was used to record phenotypes and provide leaf angle measurements, and samples were collected to measure the RWC and  $F_v/F_m$ . Data are presented as means  $\pm$  SEM, three biological replicates,  $n = 100$  individual plants. Scale bars: 1 mm. Asterisks indicate significant differences from the control group (\* $p < 0.05$ , \*\* $p < 0.01$ , \*\*\* $p < 0.001$ ).

number of regenerated branches increased over time, reaching 100% at 60 days of recovery, with a maximum of  $3.24 \pm 0.23$  regenerated branches per plant (Figures 4B–4D). At radiation doses of 500 and 1,000 Gy, the number of new regenerated branches after 7 days of recovery was  $2.96 \pm 0.14$  and  $2.86 \pm 0.16$ , respectively (Figure 4C). By 60 days of recovery, the regenerated branches had grown larger, and the number of regenerated branches was greater than in the control group for each dose, with  $4.08 \pm 0.21$  and  $3.57 \pm 0.18$  for the 500- and 1,000-Gy treatment, respectively. The regeneration rate following both treatments was 100%. Thus, 500-Gy radiation strongly promoted the regeneration of new branches (Figure 4D). When the radiation dose was increased to 2,000 Gy, regeneration was delayed, and new branches did not emerge until after 14 days of recovery (Figure 4B). A lower average number of regenerated branches ( $0.52 \pm 0.12$ ) was detected at this time (compared to the other treatments), although the number of regenerated branches increased to  $2.03 \pm 0.16$ , with a regeneration rate of 90%, after 60 days of recovery (Figures 4C and 4D).

At a radiation dose of 4,000 Gy, the moss samples exhibited signs of stress, with leaves gradually turning yellow after 3 days of recovery (Figure 4B). After 14 days of recovery, new branches started to regenerate (average of  $0.22 \pm 0.12$ ). At 60 days of recovery, the average number of branches reached  $1.20 \pm 0.15$ , with a 70% regeneration rate (Figures 4C and 4D). Radiation doses of 8,000 and 16,000 Gy caused severe damage to the moss samples; the leaves

turned yellow and died without generating new branches (Figures 4B–4D), and photosynthetic activity was undetectable. Based on these results, we estimated that the LD<sub>50</sub> (lethal dose at which 50% of the organisms survived) occurred after 1 h of treatment (LD<sub>50/1h</sub>) at ~5,000 Gy. Furthermore, when fully hydrated *S. caninervis* plants were subjected to the same gamma radiation treatments (Figure S2A), they survived and regenerated, although at an LD<sub>50/16min</sub> of ~2,000 Gy; the regeneration rates and the number of newly generated branches were lower than in plants in the dry state (Figures S2B–S2D).

#### Performance of *S. caninervis* under Mars-like conditions

To gain a deeper understanding of the survival status of *S. caninervis* under more realistic combined stress conditions, we simulated the harsh environmental conditions of Mars using the Planetary Atmospheres Simulation Facility (PASF) operated by the Reliability and Environment Test Center of the National Space Science Center, Chinese Academy of Sciences (Figures 5A–5C; Table 1). The *S. caninervis* plants survived under simulated Martian conditions (Figures 5D–5F). The untreated plants had  $0.86 \pm 0.18$  regenerated branches after 3 days of cultivation, and no new branches were found in treated plants after 3 days of recovery. The number of regenerated new branches in untreated plants reached its maximum ( $3.13 \pm 0.25$ ) after 30 days of cultivation, whereas the maximum number of new branches in plants that were treated for 1, 2, 3, and 7 days and allowed to recover for 30 days was  $2.00 \pm 0.25$ ,  $2.07 \pm 0.23$ ,

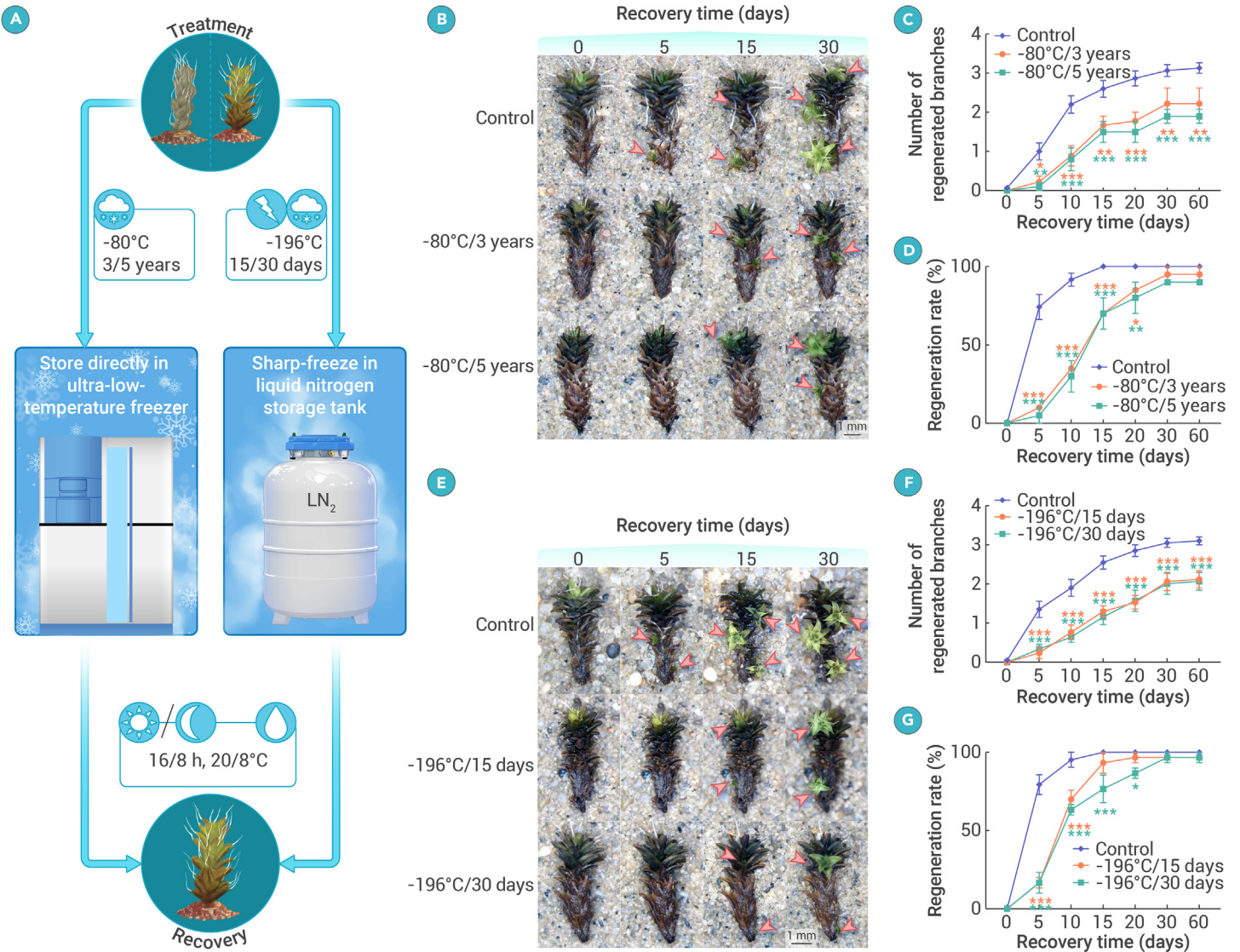


**Figure 3. Assays to determine the tolerance of *S. caninervis* to extremely low temperatures** (A) Overview of the experimental design for the low-temperature assays. Dry *S. caninervis* plants were exposed to  $-80^{\circ}\text{C}$  (in an ultra-low-temperature freezer) for 3 or 5 years or to  $-196^{\circ}\text{C}$  (in a liquid nitrogen tank) for 15 or 30 days. Subsequently, the plants were transferred to sterilized sand for recovery under a 16 h light/8 h dark cycle at a day/night temperature of  $20^{\circ}\text{C}/8^{\circ}\text{C}$ . The plants were watered every 3 days. (B) Morphological changes during the recovery period after treatment at  $-80^{\circ}\text{C}$  for 3 or 5 years. Red arrowheads indicate regenerated branches. (C and D) Number of regenerated branches on single plants (C) and regeneration rates (D) after treatment at  $-80^{\circ}\text{C}$  for 3 or 5 years. (E) Morphological changes during the recovery period after treatment at  $-196^{\circ}\text{C}$  for 15 or 30 days. Red arrows show regenerated branches. (F and G) Number of regenerated branches on single plants (F) and regeneration rates (G) after treatment at  $-196^{\circ}\text{C}$  for 15 or 30 days. Data are presented as means  $\pm$  SEM (three biological replicates,  $n = 100$  individual plants). Scale bars: 1 mm. Asterisks indicate significant differences from the control group (\* $p < 0.05$ , \*\* $p < 0.01$ , \*\*\* $p < 0.001$ ).

$1.82 \pm 0.12$ , and  $1.42 \pm 0.10$ , respectively (Figure 5E). The regeneration rate of untreated plants reached 50% after 3 days of cultivation and 100% after 15 days, whereas dry plants treated for 1, 2, 3, and 7 days required 30 days of recovery to reach a 100% regeneration rate (Figure 5F). When we subjected fully hydrated *S. caninervis* plants to Mars-like conditions for 1 day, the plants also survived and regenerated branches, although the number of branches and regeneration rate sharply decreased compared to those of dry plants (Figure S3).

## DISCUSSION

### *S. caninervis* resists various harsh conditions

*S. caninervis* is well known for its extraordinary desiccation tolerance (often known as “drying without dying”)<sup>38,39</sup>; the plants can lose more than 98% of their water and recover very rapidly after rehydration, in only seconds (Figure 2). This species is often used as a model moss to study plant desiccation tolerance. Previous studies using *S. caninervis* have focused on morphological and physiological adaptations, molecular mechanisms, and the mining of excellent stress tolerance genes.<sup>40–44</sup> In this study, we determined that *S. caninervis* also has remarkable freezing resistance, retaining its regenerative ability after being preserved at  $-80^{\circ}\text{C}$  for at least 5 years

or stored in liquid nitrogen for 1 month (Figure 3). Moreover, *S. caninervis* showed superior resistance to gamma radiation, particularly when desiccated, with an  $\text{LD}_{50/1\text{h}}$  of  $\sim 5,000$  Gy (Figure 4). The  $\text{LD}_{50}$  for humans is approximately 2.5–4.5 Gy, with severe convulsions and death occurring at around 50 Gy.<sup>45</sup> Most plants can endure radiation levels no higher than 1,000 Gy.<sup>46,47</sup> Tardigrades (water bears) are well known for their remarkable radiation tolerance, surviving up to  $\text{LD}_{50/48\text{h}}$  of  $\sim 4,200$  Gy of irradiation.<sup>45,48</sup> Although 500 Gy of gamma radiation is a high dose for most plants,<sup>46,47</sup> in *S. caninervis*, this treatment promoted the regeneration of new branches compared to nonirradiated control plants. Overall, our results indicate that *S. caninervis* is among the most radiation-tolerant organisms known.

Surprisingly, *S. caninervis* plants can survive and maintain regeneration ability under simulated Mars conditions that expose them simultaneously to several key stresses: extremely low temperatures, low oxygen (95%  $\text{CO}_2$ ), desiccation, and UV radiation. Specifically, we exposed whole *S. caninervis* plants to simulated Mars conditions with UV radiation for 7 days and demonstrated that the plants could survive under these conditions and regenerate branches after 15 days of recovery. Various bacteria,<sup>11,12</sup> microscopic fungi,<sup>9,10,13</sup> cyanobacteria, and lichens also have a notable tolerance for the simulated Martian

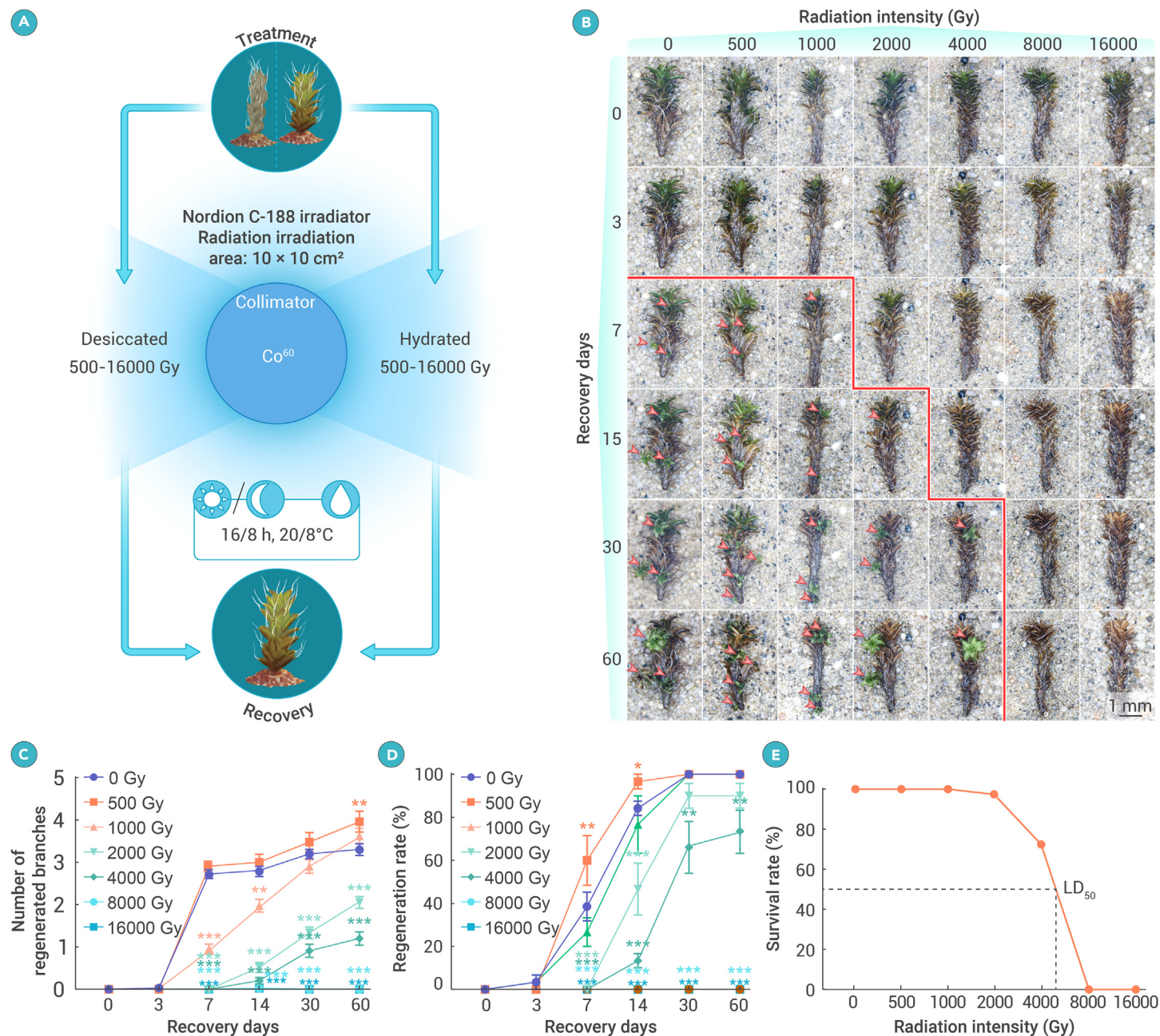


**Figure 4. Effects of gamma irradiation on the survival and regeneration of *S. caninervis* plants** (A) Schematic of the gamma irradiation experiment. Dry *S. caninervis* samples were exposed to total doses of 500–16,000 Gy using a Nordion C-188 gamma irradiator with a cylindrical source providing a concentric dose field at a dose rate of 200 rad (Si)/s. Following irradiation, the samples were rehydrated and transferred to sand for recovery and cultivation (16 h light/8 h dark, day/night temperatures of 20°C/8°C). (B) Representative images showing the phenotypic effects of gamma irradiation during recovery. Red arrowheads indicate regenerated branches. (C) Number of regenerated branches on single branches at 0, 3, 7, 14, 30, and 60 days of recovery. (D) Regeneration rates of irradiated samples. (E) Survival rates 60 days after exposure to 0, 500, 1,000, 2,000, 4,000, 8,000, or 16,000 Gy of gamma radiation. Data are presented as means  $\pm$  SEM (three biological replicates,  $n = 100$  individual plants). Scale bar: 1 mm. Asterisks indicate significant differences from the control group (0 Gy) (\* $p < 0.05$ , \*\* $p < 0.01$ , \*\*\* $p < 0.001$ ).

environment.<sup>8,14,16,49</sup> Although green plants have been poorly studied from an astrobiological perspective, a previous study demonstrated that *Funaria hygrometrica* spores and desiccated gametophytes of *Tortella squarrosa* (= *Pleurochaete squarrosa*) could withstand simulated Mars conditions for up to 2 h.<sup>50</sup> The current results demonstrate that the moss *S. caninervis* is a promising candidate for use in space exploration.

#### Possible mechanisms for the extraordinary tolerance of *S. caninervis* plants

Mosses are believed to have been the first embryophyte to colonize the land on Earth. These diminutive pioneer plants have evolved innate resistance to drought, UV radiation, and temperature fluctuations that have enabled them to adapt remarkably well to harsh aquatic-terrestrial transition zones. *S. caninervis*, a typical stress-tolerant moss, exhibits an exceptional suite of traits that allow it

to grow well in extremely harsh conditions, such as those found in desert and polar regions.<sup>30</sup> The remarkable multiple-stress tolerance of this moss arises from the intricate interplay of morphological, physiological, and molecular adaptations.<sup>30,40–44</sup>

Unique morphological features of *S. caninervis*, such as twisted leaves, conserve water by minimizing surface area and reducing transpiration, and the awns provide efficient photoprotection from intense UV radiation, extreme temperatures, and water loss.<sup>32</sup> Meanwhile, the cell wall, cell membrane, and chloroplast and its membrane structure remain intact even in a completely dehydrated state.<sup>51,52</sup> At the physiological and metabolic levels, *S. caninervis* enters a state of selective metabolic dormancy under stress conditions, strategically preserving key metabolites.<sup>31,53</sup> For example, *S. caninervis* plants maintain high levels of sucrose and maltose following stress; these sugars serve as osmotic agents and protectants that help preserve and stabilize cellular architecture. Subsequently,

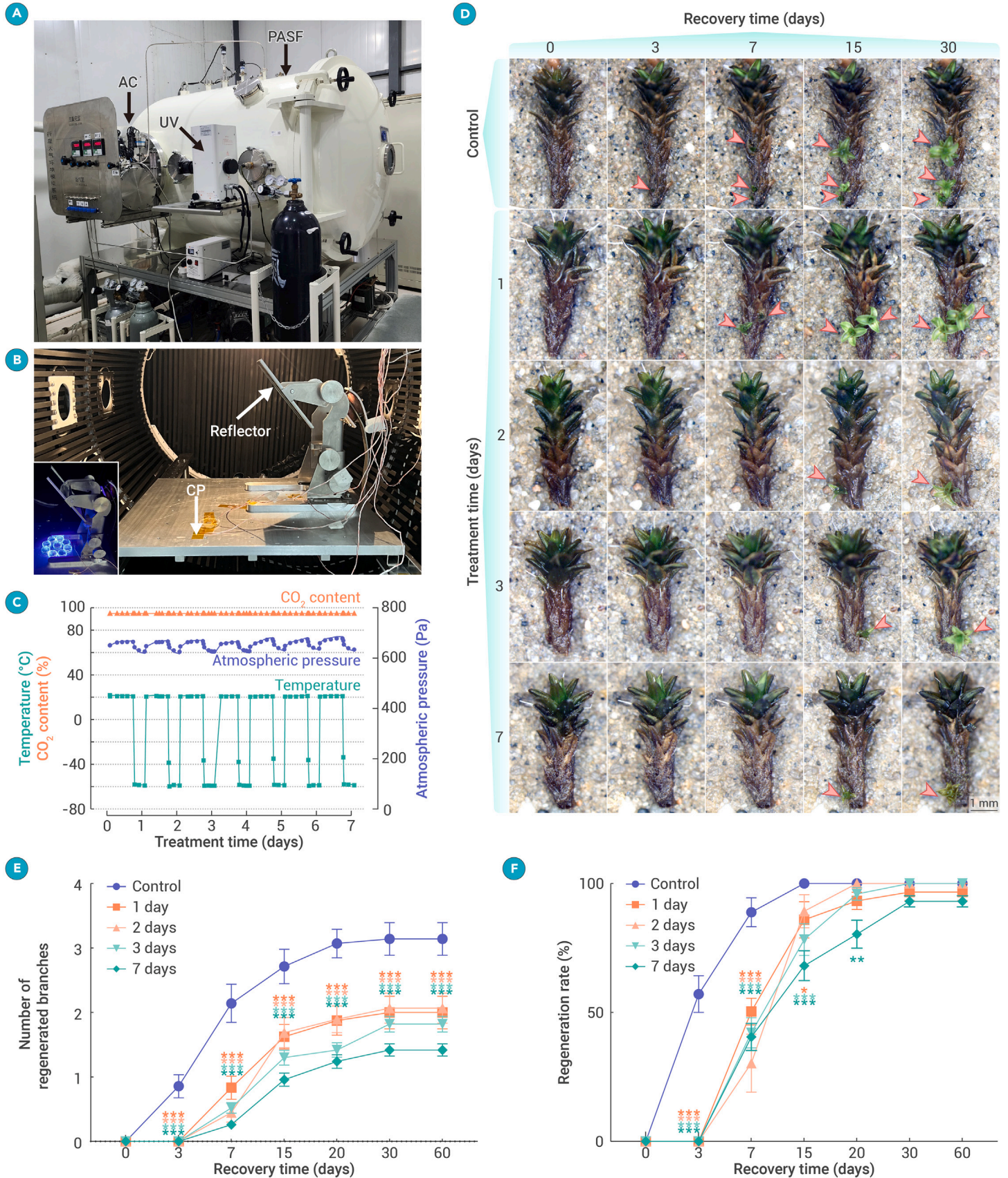


**Figure 5. Tolerance assays in a Mars-like experimental chamber** (A) General view of the Planetary Atmospheres Simulation Facility (PASF). CO<sub>2</sub>, N<sub>2</sub>, Ar, and O<sub>2</sub> can be supplied to the auxiliary chamber (AC) in specific proportions, and gas mixtures can be injected into the vacuum chamber during the experiment. The UV radiation from a 500-W mercury lamp is focused onto the glass filter and passed through a quartz glass window into the vacuum chamber. (B) The inside of the experimental chamber showing the sample holders on the plate. For low-temperature treatments, the PASF was configured with a cold plate (CP) programmed by an external controller. The inset shows how samples were exposed to UV

(legend continued on next page)

the sugars provide the energy needed for rapid recovery upon relief from stressful conditions.<sup>53</sup> Additionally, *S. caninervis* plants possess a strong ability to scavenge reactive oxygen species following stress by accumulating high levels of catalase, glutathione S-transferase, and peroxidase.<sup>54</sup> The remarkable molecular regulatory mechanisms underlying this multi-stress resilience involve the expansion of stress-related late embryogenesis abundant and catalase genes and the tandem duplication of *S. caninervis* genes encoding photoprotective early light-induced proteins.<sup>41</sup> These regulatory mechanisms also involve the selective upregulation of genes and proteins involved in critical stress response-related processes such as photosynthesis, protein stabilization, antioxidant defense, and cellular repair pathways.<sup>43,53</sup> Therefore, the multi-layered tolerance of *S. caninervis* plants to extreme stress conditions provides constitutive cellular protection under stressful conditions and enables rapid cellular repair and the recovery of physiological activity when conditions suitable for growth arise.

### Extremotolerant *S. caninervis* is a potential pioneer species for the extraterrestrial environment

Our findings provide key evidence for the extreme stress tolerance of *S. caninervis*; it can survive and retain viability in various harsh conditions and extreme Mars-like conditions in both the dry and hydrated states. Therefore, *S. caninervis* represents a promising candidate as a colonist to facilitate terraforming efforts on Mars or other planets. This is not only because *S. caninervis* is a land plant with extreme multiple stress tolerance but also because it could serve as a pioneer species and the basis for the establishment and maintenance of the ecosystem by contributing to oxygen production, carbon sequestration, and soil fertility.<sup>30,31</sup> Thus, *S. caninervis* can help drive the atmospheric, geological, and ecological processes required for other higher plants and animals while facilitating the creation of new habitable environments conducive to long-term human settlement.<sup>20,23,25,30</sup> Additionally, the superior stress tolerance of this moss could be leveraged in genetic efforts to engineer robust crop plants resilient to drought, freezing, radiation, and other extreme conditions. This will increase the ability of plants to cope with environmental changes on Earth while advancing terraforming initiatives in places such as Mars.

The exploration of outer space, including Mars, is critical for the future of humanity. Since the 1960s, multiple missions to Mars have been conducted by several countries to study the geology, mineralogy, soil, water, and ice distribution on Mars and the space environment around Mars, advancing our knowledge of the red planet to an unprecedented level.<sup>4,7,55–57</sup> Although there is still a long way to go to create self-sufficient habitats on other planets, we demonstrated the great potential of *S. caninervis*, a model moss plant, as a pioneer plant for growth on Mars. Looking to the future, we expect that this promising moss could be brought to Mars or the Moon to further test the possibility of plant colonization and growth in outer space. This challenge will require the collective efforts of scientists in a variety of disciplines, along with the integration of advanced technologies, transdisciplinary collaboration, and international cooperation.

## MATERIALS AND METHODS

### Plant materials and culture

*S. caninervis* plants were collected from the Gurbantunggut Desert of the Xinjiang Uygur Autonomous Region of China (44°32′30″ N, 88°6′42″ E). Wild *S. caninervis* plants were placed in Petri dishes and stored in the laboratory. The plants were cultured on sterilized sand collected from the desert and grown under a 16-h/8-h light/dark cycle (approximately 100  $\mu\text{mol m}^{-2} \text{s}^{-1}$  light) at 50% relative humidity and day/night temperatures of 20°C/8°C. The plants were watered with ultrapure water every 3 days. Photographs of the samples were taken under an Olympus SZX10 stereomicroscope at a fixed distance and angle.

### Dehydration and rehydration treatments

Dry wild *S. caninervis* plants were fully hydrated with ultrapure water for 24 h. Subsequently, the samples were air dried in the laboratory (~30% relative humidity, 20°C to 22°C, 100  $\mu\text{mol m}^{-2} \text{s}^{-1}$  light).<sup>43</sup> At each time point during the dehydration-rehydration (D-R) process, the RWC,  $F_v/F_m$  (optimal/maximal photochemical efficiency of photosystem II), and leaf angles of *S. caninervis* plants were measured. Images of plants were continually

recorded with a video camera to document their phenotypes. RWC curves were produced using the formula  $\text{RWC}\% = (W_f - W_d)/(W_f - W_d) \times 100$ , where  $W_f$  indicates the fresh weight measured at every time point during the D-R process,  $W_d$  indicates the weight measured after drying for 48 h at 80°C, and  $W_i$  indicates the saturated fresh weight of samples.<sup>43</sup> Plants were placed in the dark for at least 30 min, and  $F_v/F_m$  values were measured by the saturation pulse method using a portable modulated fluorometer (PAM-2500; Heinz Walz, Germany). The parameter settings were established based on guidelines provided in a previous study.<sup>31</sup> Leaf angles were measured using ImageJ software and recorded as the angle between the horizontal and the leaf axis.<sup>58</sup> Three replicates with 100 plants per replicate were used for each treatment.

### Extremely-low-temperature treatments

Both completely dry (RWC 0–2%) and fully hydrated (RWC 100%) *S. caninervis* plants were wrapped in aluminum foil and exposed directly to either –80°C in an ultra-low-temperature freezer for 3 or 5 years or –196°C in a bucket in a liquid nitrogen storage tank for 15 or 30 days. For recovery, the plants were transferred to sterilized sand and cultured under normal conditions. Plants not exposed to extremely low temperatures served as controls. Photographs were taken after 0, 5, 10, 15, 20, 30, and 60 days of recovery to document growth and development. Newly regenerated branches were defined as branches produced during the time of recovery with diameters greater than 0.1 mm.<sup>59</sup> The regeneration rate (percent) was determined as the number of *S. caninervis* plants with regenerated branches divided by the total number of *S. caninervis* plants observed. Three replicates with 100 plants per replicate were used for each treatment.

### Gamma irradiation treatment

The gamma irradiation treatments were performed using a Nordion C-188 gamma irradiator (Nordion, Canada) with an average gamma energy of 1.25 MeV. The irradiator was equipped with a cylindrical source rod, providing a concentric circular/fan-shaped dose field. The dose rate ranged from 0.00015 to 1.0 rad (Si)/s for the environmental range and from 1 to 385 rad (Si)/s for the laboratory range. The dose rate used was 200 rad (Si)/s. Completely dry (0–2% RWC) and fully hydrated (100% RWC) *S. caninervis* samples were exposed to six different doses of total gamma radiation: 500, 1,000, 2,000, 4,000, 8,000, and 16,000 Gy. The irradiation was carried out at room temperature, and the moss samples were placed in Petri dishes during treatment. Control samples were handled identically but were not exposed to gamma radiation. After gamma irradiation, the *S. caninervis* samples were fully rehydrated and cultured on sterile sand. The recovery and regeneration of the moss gametophytes were monitored at 3, 7, 14, 30, and 60 days after irradiation. At each time point, photographs were taken to document the growth and development of the moss. The newly regenerated branches were counted.<sup>59</sup> Additionally, the LD<sub>50</sub> for the irradiation of *S. caninervis* after 60 days of recovery was determined by quantifying the percentage of surviving plants compared to the nonirradiated control plants. The LD<sub>50</sub> value was estimated by interpolating the radiation intensity and survival rate data using the interp1d function from the scipy library in Python (3.10.13). Three replicates with 100 plants each were conducted for each treatment.

### Mars simulation assay

The Mars simulation experiment was conducted at the PASF operated by the Reliability and Environment Test Center of the National Space Science Center, Chinese Academy of Sciences. The PASF can simulate the characteristics of a variety of planetary surface atmospheres, including pressure, temperature, and irradiation. The simulation chamber at the PASF is a cylindrical vacuum chamber with internal dimensions of 1.2-m length and 1.0-m diameter. The chamber can reproduce a range of planetary surface conditions, including pressure ( $1 \times 10^{-3}$  to  $1 \times 10^5$  Pa) and gas composition (up to five different gases). In this study, temperature control was achieved using a cold plate that was fully programmable to provide temperatures of –60°C to +100°C. A modulated X-ray tube and high-pressure mercury lamp were used to simulate high-irradiation environments. In addition, the PASF is equipped with a Pirani-Penning combined sensor, a capacitance gauge, and a residual gas analyzer (model e-Vision2, MKS, USA) to monitor pressure and gas composition. In this experiment, the PASF was used to simulate the atmospheric pressure and gas composition of Mars, along with diurnal temperature changes and UV irradiation. The device parameters are provided in Table 1. Completely dry (0–2% RWC) *S. caninervis* plants were placed in the PASF on a cold plate and treated for 1, 2, 3, and 7 days, and fully hydrated (100% RWC) *S. caninervis* plants were treated for 1 day. Control samples were handled

radiation via a reflector. (C) Mars-like environmental profile showing the temperature, CO<sub>2</sub> content, and atmospheric pressure in the experimental chamber. (D) Morphological observation during the recovery period (16 h light/8 h dark, day/night temperatures of 20°C/8°C) after 1, 2, 3, and 7 days of treatment with simulated Martian conditions. Red arrowheads show regenerated branches. (E and F) Number of regenerated branches on single plants (E) and regeneration rates (F) after treatment. Data are presented as means  $\pm$  SEM (three biological replicates, n = 100 individual plants). Scale bar: 1 mm. Asterisks indicate significant differences from the control group (\*p < 0.05, \*\*p < 0.01, \*\*\*p < 0.001).



**Table 1.** Conditions used in the Mars simulation experiment compared to surface conditions on Mars

Parameter	Mars-like conditions in this study <sup>15,16</sup>	Mars surface conditions <sup>36,37</sup>
Pressure	650 ± 30 Pa	680–790 Pa
Temperature	(night –60°C to day +20°C), simulation of equatorial to mid-latitude regions	mean value (–55°C, –130 °C at the poles to +27°C in equatorial regions)
Atmospheric gas composition	CO <sub>2</sub> (95%), N <sub>2</sub> (3%), Ar (1.5%), and O <sub>2</sub> (0.5%)	CO <sub>2</sub> (95.97%), N <sub>2</sub> (1.89%), Ar (1.93%), and O <sub>2</sub> (0.15%)
Radiation	mercury lamp, UVC (200–280 nm), UVB (280–320 nm), and UVA (320–400 nm) at rates of 1.6, 21.5, and 39.2 W/m <sup>2</sup> , respectively	UVC (200–280 nm), UVB (280–320 nm), and UVA (320–400 nm) at rates of 3.18, 8.38, and 38.39 W/m <sup>2</sup> , respectively

identically except that they were not exposed to Mars-like conditions. For recovery, the plants were rehydrated and transferred to sterilized sand for culture under normal conditions. Photographs were taken after 0, 3, 7, 15, 20, 30, and 60 days of recovery culture to document the growth and development of the moss. Three replicates with 100 plants each were used for each treatment.

### Statistical analysis

All data are presented as means ± standard error of the mean (SEM) with  $n = 100$  samples per group. All statistical analyses were conducted using GraphPad Prism software (v.9.0) with one-way ANOVA followed by Dunnett's multiple-comparisons test. Differences were considered statistically significant at  $*p < 0.05$ ,  $**p < 0.01$ , and  $***p < 0.001$ . All figures were generated using GraphPad Prism 9 and Adobe Illustrator CS6 software.

### REFERENCES

- Cabrol, N.A. (2021). Tracing a modern biosphere on Mars. *Nat. Astron.* **5**(3): 210–212.
- Levchenko, I., Xu, S., Mazouffre, S., et al. (2019). Mars colonization: Beyond getting there. *Glob. Chall.* **3**(1): 1800062. <https://doi.org/10.1002/gch2.201800062>.
- Mi, L. (2020). What's next for key and core tech? *Innovation* **1**(1): 100015. <https://doi.org/10.1016/j.xinn.2020.04.015>.
- Farley, K.A., Williford, K.H., Stack, K.M., et al. (2020). Mars 2020 mission overview. *Space Sci. Rev.* **216**(8): 142. <https://doi.org/10.1007/s11214-020-00762-y>.
- Grotzinger, J.P., Crisp, J., Vasavada, A.R., et al. (2012). Mars science laboratory mission and science investigation. *Space Sci. Rev.* **170**(1-4): 5–56. <https://doi.org/10.1007/s11214-012-9892-2>.
- Walsh, K.J., Morbidelli, A., Raymond, S.N., et al. (2011). A low mass for Mars from Jupiter's early gas-driven migration. *Nature* **475**(7355): 206–209. <https://doi.org/10.1038/nature10201>.
- Zheng, Y.C. (2020). Mars exploration in 2020. *Innovation* **1**(2): 100036. <https://doi.org/10.1016/j.xinn.2020.100036>.
- Çelekli, A., and Zariç, Ö.E. (2024). Breathing life into Mars: Terraforming and the pivotal role of algae in atmospheric genesis. *Life Sci. Space Res.* **41**: 181–190. <https://doi.org/10.1016/j.lssr.2024.03.001>.
- Horneck, G., Moeller, R., Cadet, J., et al. (2012). Resistance of bacterial endospores to outer space for planetary protection purposes—experiment PROTECT of the EXPOSE-E mission. *Astrobiology* **12**(5): 445–456. <https://doi.org/10.1089/ast.2011.0737>.
- Zakharova, K., Marzban, G., de Vera, J.P., et al. (2014). Protein patterns of black fungi under simulated Mars-like conditions. *Sci. Rep.* **4**: 5114. <https://doi.org/10.1038/srep05114>.
- Liu, J., Zhang, W., He, K., et al. (2022). Survival of the magnetotactic bacterium *Magnetospirillum gryphiswaldense* exposed to Earth's lower near space. *Sci. Bull.* **67**(13): 1335–1339. <https://doi.org/10.1016/j.scib.2022.03.005>.
- Musilova, M., Wright, G., Ward, J.M., et al. (2015). Isolation of radiation-resistant bacteria from Mars analog antarctic dry valleys by preselection, and the correlation between radiation and desiccation resistance. *Astrobiology* **15**(12): 1076–1090. <https://doi.org/10.1089/ast.2014.1278>.
- Onofri, S., de Vera, J.P., Zucconi, L., et al. (2015). Survival of antarctic cryptoendolithic fungi in simulated Martian conditions on board the international space station. *Astrobiology* **15**(12): 1052–1059. <https://doi.org/10.1089/ast.2015.1324>.
- de Vera, J.P., Möhlmann, D., Butina, F., et al. (2010). Survival potential and photosynthetic activity of lichens under Mars-like conditions: A laboratory study. *Astrobiology* **10**(2): 215–227. <https://doi.org/10.1089/ast.2009.0362>.
- Lorenz, C., Bianchi, E., Poggiali, G., et al. (2023). Survivability of the lichen *Xanthoria parietina* in simulated Martian environmental conditions. *Sci. Rep.* **13**(1): 4893. <https://doi.org/10.1038/s41598-023-32008-6>.
- Noetzel, R.D., Miller, A.Z., de la Rosa, J.M., et al. (2018). Cellular responses of the lichen in Mars-like conditions. *Front. Microbiol.* **9**: 308. <https://doi.org/10.3389/fmicb.2018.00308>.
- Weber, B., Belnap, J., Büdel, B., et al. (2022). What is a biocrust? A refined, contemporary definition for a broadening research community. *Biol. Rev.* **97**(5): 1768–1785. <https://doi.org/10.1111/brv.12862>.
- Delgado-Baquerizo, M., Maestre, F.T., Eldridge, D.J., et al. (2016). Biocrust-forming mosses mitigate the negative impacts of increasing aridity on ecosystem multifunctionality in drylands. *New Phytol.* **209**(4): 1540–1552. <https://doi.org/10.1111/nph.13688>.
- Ferrenberg, S., and Reed, S.C. (2017). Biocrust ecology: Unifying micro- and macro-scales to confront global change. *New Phytol.* **216**(3): 643–646. <https://doi.org/10.1111/nph.14826>.
- Rodriguez-Caballero, E., Belnap, J., Büdel, B., et al. (2018). Dryland photoautotrophic soil surface communities endangered by global change. *Nat. Geosci.* **11**(3): 185–189. <https://doi.org/10.1038/s41561-018-0072-1>.
- Zhang, Y.M., Chen, J., Wang, L., et al. (2007). The spatial distribution patterns of biological soil crusts in the Gurbantunggut Desert, Northern Xinjiang, China. *J. Arid Environ.* **68**(4): 599–610. <https://doi.org/10.1016/j.jaridenv.2006.06.012>.
- Duniway, M.C., Pfennigwerth, A.A., Fick, S.E., et al. (2019). Wind erosion and dust from US drylands: A review of causes, consequences, and solutions in a changing world. *Ecosphere* **10**(3): e02650. <https://doi.org/10.1002/ecs2.2650>.
- Eldridge, D.J., Reed, S., Travers, S.K., et al. (2020). The pervasive and multifaceted influence of biocrusts on water in the world's drylands. *Glob. Chang. Biol.* **26**(10): 6003–6014. <https://doi.org/10.1111/gcb.15232>.
- Phillips, M.L., McNellis, B.E., Howell, A., et al. (2022). Biocrusts mediate a new mechanism for land degradation under a changing climate. *Nat. Clim. Chang.* **12**(1): 71–76. <https://doi.org/10.1038/s41558-021-01249-6>.
- Elbert, W., Weber, B., Burrows, S., et al. (2012). Contribution of cryptogamic covers to the global cycles of carbon and nitrogen. *Nat. Geosci.* **5**(7): 459–462. <https://doi.org/10.1038/ngeo1486>.
- Zhou, X., Tao, Y., Yin, B., et al. (2020). Nitrogen pools in soil covered by biological soil crusts of different successional stages in a temperate desert in Central Asia. *Geoderma* **366**: 114166. <https://doi.org/10.1016/j.geoderma.2019.114166>.
- Bowker, M.A., Reed, S.C., Maestre, F.T., et al. (2018). Biocrusts: The living skin of the earth. *Plant Soil* **429**(1-2): 1–7. <https://doi.org/10.1007/s11104-018-3735-1>.
- Chamizo, S., Cantón, Y., Miralles, I., et al. (2012). Biological soil crust development affects physicochemical characteristics of soil surface in semiarid ecosystems. *Soil Biol. Biochem.* **49**: 96–105. <https://doi.org/10.1016/j.soilbio.2012.02.017>.
- Sun, F., Xiao, B., Li, S., et al. (2021). Towards moss biocrust effects on surface soil water holding capacity: Soil water retention curve analysis and modeling. *Geoderma* **399**: 115120. <https://doi.org/10.1016/j.geoderma.2021.115120>.
- Yin, B., Zhang, Y., Zhang, H., et al. (2023). Phylogeographic structure of *Syntrichia caninervis* Mitt, a xerophytic moss, highlights the expanded during glacial period. *J. Plant Ecol.* **16**(2): rtac057. <https://doi.org/10.1093/jpe/rtac057>.
- Zhang, J., Zhang, Y.M., Downing, A., et al. (2011). Photosynthetic and cytological recovery on re moistening *Syntrichia caninervis* Mitt., a desiccation-tolerant moss from Northwestern China. *Photosynthetica* **49**(1): 13–20. <https://doi.org/10.1007/s11099-011-0002-6>.
- Pan, Z., Pitt, W.G., Zhang, Y., et al. (2016). The upside-down water collection system of *Syntrichia caninervis*. *Nat. Plants* **2**(7): 16076. <https://doi.org/10.1038/nplants.2016.76>.
- Yin, B., Li, J., Zhang, Q., et al. (2021). Freeze-thaw cycles change the physiological sensitivity of *Syntrichia caninervis* to snow cover. *J. Plant Physiol.* **266**: 153528. <https://doi.org/10.1016/j.jplph.2021.153528>.
- Yin, B.F., and Zhang, Y.M. (2016). Physiological regulation of *Syntrichia caninervis* Mitt. in different microhabitats during periods of snow in the Gurbantunggüt Desert, Northwestern China. *J. Plant Physiol.* **194**: 13–22. <https://doi.org/10.1016/j.jplph.2016.01.015>.
- Zhang, J., and Zhang, Y. (2020). Ecophysiological responses of the biocrust moss *Syntrichia caninervis* to experimental snow cover manipulations in a temperate desert of central Asia. *Ecol. Res.* **35**(1): 198–207. <https://doi.org/10.1111/1440-1703.12072>.
- Hassler, D.M., Zeitzlin, C., Wimmer-Schweingruber, R.F., et al.; MSL Science Team (2014). Mars' surface radiation environment measured with the Mars science laboratory's Curiosity Rover. *Science* **343**(6169): 1244797. <https://doi.org/10.1126/science.1244797>.
- Jiang, C., Jiang, Y., Li, H., et al. (2023). Initial results of the meteorological data from the first 325 sols of the Tianwen-1 mission. *Sci. Rep.* **13**(1): 3325. <https://doi.org/10.1038/s41598-023-30513-2>.
- Farrant, J.M., and Hilhorst, H.W.M. (2021). What is dry? Exploring metabolism and molecular mobility at extremely low water contents. *J. Exp. Bot.* **72**(5): 1507–1510.
- Oliver, M.J., Farrant, J.M., Hilhorst, H.W.M., et al. (2020). Desiccation tolerance: Avoiding cellular damage during drying and rehydration. *Annu. Rev. Plant Biol.* **71**: 435–460. <https://doi.org/10.1146/annurev-arplant-071219-105542>.
- Li, X., Yang, R., Liang, Y., et al. (2023). The *ScAPD1-like* gene from the desert moss *Syntrichia caninervis* enhances resistance to *Verticillium dahliae* via phenylpropanoid gene regulation. *Plant J.* **113**(1): 75–91. <https://doi.org/10.1111/tpj.16035>.

41. Silva, A.T., Gao, B., Fisher, K.M., et al. (2021). To dry perchance to live: Insights from the genome of the desiccation-tolerant biocrust moss *Syntrichia caninervis*. *Plant J.* **105**(5): 1339–1356. <https://doi.org/10.1111/tpj.15116>.
42. Yang, H., Bozorov, T.A., Chen, X., et al. (2021). Yield comparisons between cotton variety Xin Nong Mian 1 and its transgenic *ScALDH21* lines under different water deficiencies in a desert-oasis ecotone. *Agronomy-Basel* **11**(5): 1019. <https://doi.org/10.3390/agronomy11051019>.
43. Yang, R., Li, X., Yang, Q., et al. (2023). Transcriptional profiling analysis providing insights into desiccation tolerance mechanisms of the desert moss *Syntrichia caninervis*. *Front. Plant Sci.* **14**: 1127541. <https://doi.org/10.3389/fpls.2023.1127541>.
44. Zhang, Y., Zhang, Y., Wang, C., et al. (2024). Enhancement of salt tolerance of alfalfa: Physiological and molecular responses of transgenic alfalfa plants expressing *Syntrichia caninervis*-derived ScABI3. *Plant Physiol. Bioch.* **207**: 108335. <https://doi.org/10.1016/j.plaphy.2024.108335>.
45. Kasianchuk, N., Rzymyski, P., and Kaczmarek, Ł. (2023). The biomedical potential of tardigrade proteins: A review. *Biomed. Pharmacother.* **158**: 114063. <https://doi.org/10.1016/j.biopha.2022.114063>.
46. Jan, S., Parween, T., Siddiqi, T.O., et al. (2012). Effect of gamma radiation on morphological, biochemical, and physiological aspects of plants and plant products. *Environ. Rev.* **20**(1): 17–39. <https://doi.org/10.1139/A11-021>.
47. Wi, S.G., Chung, B.Y., Kim, J.S., et al. (2007). Effects of gamma irradiation on morphological changes and biological responses in plants. *Micron* **38**(6): 553–564. <https://doi.org/10.1016/j.micron.2006.11.002>.
48. Beltrán-Pardo, E., Jönsson, K.I., Harms-Ringdahl, M., et al. (2015). Tolerance to gamma radiation in the tardigrade *Hypsibius dujardini* from embryo to adult correlate inversely with cellular proliferation. *PLoS One* **10**(7): e0133658. <https://doi.org/10.1371/journal.pone.0133658>.
49. Armstrong, R.A. (2021). The potential of pioneer lichens in terraforming Mars. In *Terraforming Mars* (Scrivener Publishing LLC), pp. 533–553. <https://doi.org/10.1002/9781119761990.ch21>.
50. Gomez, J.M.G., Estebanez, B., Sanzarranz, A., et al. (2016). Survival of moss reproductive structures under simulated Martian environmental conditions and extreme thermal stress: Vibrational spectroscopic study and astrobiological implications. *OMICS Int.* **4**(2): 1000151. <https://doi.org/10.4172/2332-2519.1000151>.
51. Mao, Y., Liu, W., Yang, X., et al. (2022). *Syntrichia caninervis* adapt to mercury stress by altering submicrostructure and physiological properties in the Gurbantünggüt Desert. *Sci. Rep.* **12**(1): 11717. <https://doi.org/10.1038/s41598-022-15822-2>.
52. Wu, N., Zhang, Y.M., Downing, A., et al. (2012). Membrane stability of the desert moss *Syntrichia caninervis* Mitt. during desiccation and rehydration. *J. Bryol.* **34**: 1–8. <https://doi.org/10.1179/1743282011y.0000000043>.
53. Yang, Q., Yang, R., Gao, B., et al. (2023). Metabolomic analysis of the desert moss *Syntrichia caninervis* provides insights into plant dehydration and rehydration response. *Plant Cell Physiol.* **64**(11): 1419–1432. <https://doi.org/10.1093/pcp/pcad110>.
54. Salih, H., Bai, W.W., Liang, Y.Q., et al. (2024). ROS scavenging enzyme-encoding genes play important roles in the desert moss *Syntrichia caninervis* response to extreme cold and desiccation stresses. *Int. J. Biol. Macromol.* **254**: 127778. <https://doi.org/10.1016/j.ijbiomac.2023.127778>.
55. Bennett, K.A., Fox, V.K., Bryk, A., et al. (2023). The Curiosity Rover's exploration of Glen Torridon, Gale Crater, Mars: An overview of the campaign and scientific results. *J. Geophys. Res-Planet* **128**(1): e2022JE007185. <https://doi.org/10.1029/2022JE007185>.
56. Li, C.L., Zhang, R.Q., Yu, D.Y., et al. (2021). China's Mars exploration mission and science investigation. *Space Sci. Rev.* **217**(4): 57. <https://doi.org/10.1007/s11214-021-00832-9>.
57. Tian, H., Zhang, T., Jia, Y., et al. (2021). Zhurong: Features and mission of China's first Mars rover. *Innovation* **2**(3): 100121. <https://doi.org/10.1016/j.xinn.2021.100121>.
58. Wu, N., Zhang, Y.M., Downing, A., et al. (2014). Rapid adjustment of leaf angle explains how the desert moss, *Syntrichia caninervis*, copes with multiple resource limitations during rehydration. *Funct. Plant Biol.* **41**(2): 168–177. <https://doi.org/10.1071/Fp13054>.
59. Liu, X., Zhou, P., Li, X., et al. (2021). Propagation of desert moss *Syntrichia caninervis* in peat pellet: A method for rapidly obtaining large numbers of cloned gametophytes. *Plant Methods* **17**(1): 42. <https://doi.org/10.1186/s13007-021-00740-7>.

## ACKNOWLEDGMENTS

This work was supported by the Key Research Program of Frontier Sciences, Chinese Academy of Sciences (ZDBS-LY-SM009), the Leading Talents in Technological Innovation Program (2022TSYCLJ0049), and The Third Xinjiang Scientific Expedition Program (grants 2022xjkk0202 and 2021xjkk0500).

## AUTHOR CONTRIBUTIONS

All authors have made substantial, direct, and intellectual contributions to the work discussed in this publication. X.L., Y.Z., and D.Z. conceived and designed the project. W.B., Q.Y., and B.Z. performed the experiments. X.L., W.B., Q.Y., B.Y., and Z.Z. analyzed the data and wrote the draft. X.L., Y.Z., D.Z., and T.K. discussed the data and revised the manuscript. All authors read and approved the final manuscript.

## DECLARATION OF INTERESTS

The authors declare no competing interest.

## SUPPLEMENTAL INFORMATION

It can be found online at <https://doi.org/10.1016/j.xinn.2024.100657>.

## LEAD CONTACT WEBSITE

[http://egi.cas.cn/sourcedb/zw/zjrc/yjy/200908/t20090805\\_2330208.html](http://egi.cas.cn/sourcedb/zw/zjrc/yjy/200908/t20090805_2330208.html)  
[http://egi.cas.cn/sourcedb/zw/zjrc/yjy/200908/t20090805\\_2330188.html](http://egi.cas.cn/sourcedb/zw/zjrc/yjy/200908/t20090805_2330188.html)  
[http://ib.cas.cn/sourcedb/cn/expert/200904/t20090407\\_45025.html](http://ib.cas.cn/sourcedb/cn/expert/200904/t20090407_45025.html)